A Loss of Innocence? Charge-Transfer Interactions with $Ph_3PNPPh_3^+$ as Electron Acceptor

Mats Tilset,*,† Andrei A. Zlota,‡ Kirsten Folting,‡ and Kenneth G. Caulton*,‡

Contribution from the Department of Chemistry, University of Oslo, P.O. Box 1033, Blindern, N-0315 Oslo, Norway, and Department of Chemistry and Molecular Structure Center, Indiana University, Bloomington, Indiana 47405

Received July 27, 1992

Abstract: Comparison of $[Cat][CpCr(CO)_2PEt_3]$ (Cat = Et_4N^+ and $Ph_3PNPPh_3^+$ (PPN^+)) by NMR, visible/UV, and infrared spectroscopy in CH_3CN and in THF shows that ion pairing for the PPN complex occurs in THF, and that such pairing involves a detectable amount of charge transfer from anion to cation. This causes a rise in the CO stretching frequencies, which can be compared to the values in the fully-oxidized species $CpCr(CO)_2(PEt_3)^\bullet$. The crystal structure of both compounds shows a decrease in ∠C–Cr–C to be the most evident consequence of charge transfer.

Introduction

The Kochi group has extensively developed the concept of charge-transfer complexes between electron acceptors and organometallic electron donors.[1-3] The latter are always electron-rich, easily-oxidized species. They are *sometimes* anionic, but the "charge-transfer complex" concept clearly transcends cation/anion pairs.[4] The more potent electron acceptors are olefins and polyenes heavily substituted with electron-withdrawing substituents (e.g., CN), but it has been shown that even electron-precise (i.e., 18-valence electron) cations such as Cp_2Co^+ can form charge-transfer complexes (with $Co(CO)_4^-$, for example). However, both transition-metal carbonylate chemists[5,6] and the recent work of the Kochi group consider the PPN cation, $Ph_3P{=}N{=}PPh_3^+$, as the limiting case of a charge-delocalized, noninteracting cation. We report here results which show the limitations on this idealization and ultimately lead to a better understanding of the relationship between charge-transfer interaction and ion pairing.

In the course of a study[7] of the electrochemistry of a series of anions $CpCr(CO)_2L^-$ (L = CO, PPh_3, PEt_3), we had occasion to synthesize solid compounds of these anions with both Et_4N^+ and $Ph_3PNPPh_3^+$ (PPN^+) cations. It was surprising to us that these cations gave yellow and deep red solids, respectively, and that the intensity of the red color increased from L = CO to L = PEt_3. Kochi has shown[1-3] that such colors in salts containing not only Cp_2Co^+ but also quaternized aromatic amines are due to charge transfer from anion to cation. However, since both Et_4N^+ and PPN^+ are generally taken as noninteracting and nonperturbing cations,[1,5,8-10a] our observations were wholly unanticipated. The PPN^+ counterion is currently assumed to be quite "innocent" in its salts.[10b] The red color of the PPN^+ salts persists in THF solution, but it is absent (in fact, pale yellow) in CH_3CN solvent. The cyclic voltammetry of salts of both cations are identical in CH_3CN/Bu_4NPF_6. We therefore felt it important to characterize the solid-state structure of a pair of such compounds, to look both for differences in the structure of the anion and also for some specific cation/anion interactions in $[PPN][CpCr(CO)_2PEt_3]$.

Experimental Section

General Procedures. All manipulations involving organometallic compounds were carried out with use of vacuum-line, Schlenk, syringe, or drybox techniques. Acetonitrile and acetonitrile-d_3 were distilled from P_2O_5 and CaH_2, respectively. Ether and THF used for syntheses and electrochemical experiments were distilled from sodium benzophenone ketyl. THF for spectroscopic use was distilled from potassium metal. The electrochemical instrumentation, cells, data handling procedures, and electrodes have been previously described.[11] When used as the solvent for electrochemical experiments, acetonitrile containing 0.1 M $Bu_4N^+PF_6^-$ was passed through a column of active neutral alumina before use to remove water and protic impurities. The electrolyte was freed of air by purging with purified argon, and all measurements and electrolyses were carried out under a blanket of solvent-saturated argon at 293 K. ^1H NMR spectra were recorded on Nicolet 360, Varian XL-300, or Varian Gemini-200 instruments on 0.1 M solutions. ^1H NMR chemical shifts are reported in ppm relative to tetramethylsilane, with the residual solvent proton resonances as internal standards (δ 1.93 for acetonitrile-d_3; δ 3.58 for THF-d_8). ^{31}P NMR chemical shifts were referenced externally to 85% H_3PO_4 at 0.00 ppm with shifts downfield of the reference considered positive. Infrared spectra were obtained on a Perkin-Elmer 1310 infrared spectrophotometer. Elemental analyses were performed by Ilse Beetz Mikroanalytisches Laboratorium, Kronach, Germany. Multiple analyses of the same sample showed some variation. We report typical values here (some involving poor agreement) from simultaneous analysis of a single submitted sample.

Pentamethylcyclopentadiene,[12] $CpCr(CO)_3^-Et_4N^+$,[13] and $CpCr(CO)_3^-PPN^+$ [14] were synthesized according to published procedures. $PPN^+PF_6^-$ was precipitated by the addition of 60% HPF_6 to an aqueous solution of PPN^+Cl^-, followed by extraction with and recrystallization from dichloromethane/ether.

Fresh THF solutions of $CpCr(CO)_3H$ were made by acidification of $CpCr(CO)_3^-Na^+$ (prepared from $Cr(CO)_3(NCMe)_3$ and cyclopentadienylsodium) with 1 equiv of trifluoroacetic acid. Except for $[PPN][CpCr(CO)_3]$ and $[Et_4N][CpCr(CO)_3]$, the product chromium carbonyl anions were moderately to extremely air sensitive in the solid state.

NMR Spectra. Since our solution manipulation (e.g., recrystallization) of these salts showed them to be extremely sensitive, we took a variety

† University of Oslo.
‡ Indiana University.

(1) Kochi, J. K.; Bockman, T. M. *Adv. Organomet. Chem.* **1991**, *33*, 52.
(2) Bockman, T. M.; Kochi, J. K. *J. Am. Chem. Soc.* **1989**, *111*, 4669.
(3) Organometallic Radical Processes; Trogler, W. C., Ed.; Elsevier: Amsterdam, 1990.
(4) Kochi, J. K. *Acta Chem. Scand.* **1990**, *44*, 409.
(5) Darensbourg, M. Y. *Prog. Inorg. Chem.* **1985**, *33*, 221.
(6) Darensbourg, M. Y.; Barros, H.; Borman, C. *J. Am. Chem. Soc.* **1977**, *99*, 1647.
(7) Tilset, M. *J. Am. Chem. Soc.* **1992**, *114*, 2740.
(8) Svorstol, I.; Hoiland, H.; Songstad, J. *Acta Chem. Scand., Ser. B* **1984**, *B38*, 885.
(9) Mingos, D. M.; Rohl, A. L. *J. Chem. Soc., Dalton Trans.* **1991**, 3419.
(10) (a) Braga, D.; Grepioni, F. *Organometallics* **1992**, *11*, 1256. (b) See, however, Darensbourg, D. J.; Rheingold, A. L. *Inorg. Chem.* **1986**, *25*, 125.
(11) (a) Ahlberg, E.; Parker, V. D. *J. Electroanal. Chem. Interfacial Electrochem.* **1981**, *121*, 57. (b) Ahlberg, E.; Parker, V. D. *J. Electroanal. Chem. Interfacial Electrochem.* **1981**, *121*, 73. (c) Ahlberg, E.; Parker, V. D. *Acta Chem. Scand., Ser. B* **1980**, *B34*, 97.
(12) Threlkel, R. S.; Bercaw, J. E.; Seidler, P. F.; Stryker, J. M.; Bergman, R. G. *Org. Synth.* **1987**, *65*, 42.
(13) Behrens, U.; Edelmann, F. *J. Organomet. Chem.* **1984**, *263*, 179.
(14) Lai, C.-K.; Feighery, W. G.; Zhen, Y.; Atwood, J. D. *Inorg. Chem.* **1989**, *28*, 3929.

0002-7863/93/1515-4113$04.00/0

of approaches to prepare samples for NMR spectroscopy. All solid was multiply recrystallized and the solid used was crystalline. All glassware was silylated with 1,1,1,3,3,3-hexamethyldisilazane (Aldrich, 98%). One set of studies employed vacuum transfer of predried/degassed solvents onto solid in tubes sealed with a threaded Teflon valve closure. Another set of studies used vacuum transfer of solvent into tubes already loaded with crystalline sample, followed by flame sealing of the tube. In every case, work was done at night in rooms illuminated only by remote fluorescent lights. Solutions in NMR tubes were wrapped in aluminum foil and exposure to (weak) light was less than 20 s.

Our best THF-d_8 (or CD_3CN) samples of $[PPN][CpCr(CO)_2PEt_3]$ reproducibly showed broadening (~2.5-ppm full width at half-height) of *only* the Cr/PEt_3 $^{31}P\{^1H\}$ NMR signal when *freshly* prepared. ^1H NMR signals were sharp, however. The extent of this line broadening was variable from sample to sample, depending on sample history. $[Et_4N][CpCr(CO)_2PEt_3]$ does not show such broadening. The chemical shift is unaltered when the line broadening is present. However, even 5 min of exposure to fluorescent (room) light in a sealed tube sharpens this line completely, with production of no new ^{31}P NMR signals. This sharp spectrum then remains unchanged for at least 2 days in the absence of further irradiation. We therefore propose that our recrystallization plus NMR sample preparation process together yields $\sim 10^{-2}$% of the persistent radical $CpCr(CO)_2PEt_3$ and that electron self-exchange between this and the related monoanion gives rise to the observed ^{31}P NMR line broadening. Photolysis then irreversibly converts the radical to diamagnetic products (e.g., $Cp_2Cr_2(CO)_n(PEt_3)_{4-n}$ or $[CpCr(CO)_2(PEt_3)_2]$-$[CpCr(CO)_2(PEt_3)]$), thus eliminating the catalytic source of the dynamic line broadening. To pursue this hypothesis, we have prepared a ^{31}P NMR sample of $[PPN][CpCr(CO)_2PEt_3]$ under conditions identical to those above but with the addition of 2 mg of elemental sodium in the presence of 10 mg of naphthalene (intended to reduce $CpCr(CO)_2PEt_3$ to its anion). The resulting $^{31}P\{^1H\}$ NMR spectrum shows a sharp peak due to coordinated PEt_3.

In CD_3CN, the ^1H NMR chemical shifts are independent of cation, so data are given for only one salt. The ^1H NMR signals of the cation in CD_3CN were invariant to anion and are given only once. PPN^+: 7.4–7.8 (m, 30H). Et_4N^+: 1.20 (tt, J = 7.2, 1.8 Hz, 12H), 3.15 (q, J = 7.2 Hz, 8H).

$Cp^*Cr(CO)_3$-PPN$^+$ (1b(PPN)). $Cr(CO)_3(NCMe)_3$ (prepared from $Cr(CO)_6$ (330 mg, 1.50 mmol)) was treated with pentamethylcyclopentadiene (250 mg, 1.85 mmol) in THF (20 mL) at reflux for 2 h. The solvent was removed by vacuum transfer, and the residue was sublimed at ca. 10^{-3} Torr at 60–70 °C. The resulting mixture (270 mg, 1.00 mmol) of $Cp^*Cr(CO)_3H$ and $(Cp^*Cr(CO)_3)_2$ was stirred with KO*t*-Bu (112 mg, 1.00 mmol) and 1% Na/Hg (ca. 0.5 mL) in THF (20 mL) overnight. The orange solution was filtered through Celite, and PPN^+Cl^- (574 mg, 1.00 mmol) was added. The suspension was stirred for 4 h, and the solution was filtered through Celite. The filtrate was concentrated to 5 mL by vacuum transfer. The product was crystallized twice by slow diffusion of ether vapors into the THF solutions to give orange-red prisms (647 mg, 53%). Anal. Calcd for $C_{49}H_{45}CrNO_3P_2$: C, 72.67; H, 5.60; N, 1.73. Found: C, 72.81; H, 5.72; N, 2.90. ^1H NMR (25 °C, CD_3CN): 1.83 (s, 15H).

$Cp^*Cr(CO)_3$-Et_4N^+ (1b(Et_4N)). The procedure was analogous to that employed for the PPN^+ salt except that $Et_4N^+Br^-$ replaced PPN^+Cl^-, and the reaction gave yellow flaky crystals (56%). Anal. Calcd for $C_{21}H_{35}CrNO_3$: C, 62.82; H, 8.79; N, 3.49. Found: C, 60.20; H, 8.38; N, 3.37.

$CpCr(CO)_2P(OMe)_3$-PPN$^+$ (1c(PPN)). To a solution of $CpCr(CO)_3H$ (from $Cr(CO)_6$ (400 mg, 1.82 mmol)) in THF (20 mL) was added $P(OMe)_3$ (215 mL, 1.82 mmol) at 0 °C. The solution was heated at reflux for 1 h, and the volatiles were removed by vacuum transfer. The residue was extracted with ether (15 mL), and the extract was filtered through Celite. The solvent was removed by vacuum transfer, and THF (10 mL) was added. Addition of KO*t*-Bu (204 mg, 1.82 mmol) caused the formation of a yellow precipitate in a yellowish-green solution. Addition of PPN^+Cl^- (1000 mg, 1.74 mmol) yielded a deep red solution that was stirred overnight. The solution was filtered through Celite, and the resulting solution was concentrated to ca. 5 mL by vacuum transfer. The product was crystallized twice by slow diffusion of ether vapor into the THF solution. Red crystals were obtained, 930 mg (64%). Anal. Calcd for $C_{46}H_{44}CrNO_5P_3$: C, 66.11; H, 5.31; N, 1.68. Found: C, 66.40; H, 5.39; N, 1.68. ^1H NMR (25 °C, CD_3CN): 3.39 (d, J = 11 Hz, 9H), 4.17 (d, J = 2 Hz, 5H).

$CpCr(CO)_2P(OMe)_3$-Et_4N^+ (1c(Et_4N)). The preparation followed the same procedure as that employed for the PPN salt except that PPN^+Cl^- was replaced with equimolar amounts of $Et_4N^+Br^-$. Light yellow crystals (75%) were obtained. Anal. Calcd for $C_{18}H_{34}CrNO_5P$: C, 50.58; H, 8.02; N, 3.28. Found: C, 50.02; H, 7.86; N, 3.47.

$CpCr(CO)_2PPh_3$-PPN$^+$ (1d(PPN)). The preparation followed the previously published procedure[15] and gave the product as reddish-black prisms (72%). Anal. Calcd for $C_{61}H_{50}CrNO_2P_3$: C, 75.22; H, 5.17; N, 1.44. Found: C, 75.36; H, 5.20; N, 1.71. ^1H NMR (25 °C, CD_3CN): 3.96 (d, J = 1.7 Hz, 5H), 7.15–7.30 (m, 9H), 7.45–7.55 (m, 6H).

$CpCr(CO)_2PPh_3$-Et_4N^+ (1d(Et_4N)). The preparation followed the procedure employed for the PPN salt except that $Et_4N^+Br^-$ replaced PPN^+Cl^-. Brown needles (62%) were obtained. Anal. Calcd for $C_{33}H_{40}CrNO_2P$: C, 70.07; H, 7.13; N, 2.48. Found: C, 70.03; H, 7.10; N, 2.86.

$CpCr(CO)_2PEt_3$-PPN$^+$ (1e(PPN)). The synthesis followed the procedure used for the $P(OMe)_3$-substituted analogue and yielded black prisms (76%). Some decomposition occurred during the crystallization procedures, and the product had to be separated from the off-white, free-flowing powder by multiple ether washings and decantations. Anal. Calcd for $C_{49}H_{50}CrNO_2P_3$: C, 70.92; H, 6.07; N, 1.69. Found: C, 70.89; H, 6.09; N, 2.66. ^1H NMR (THF-d_8): 7.5–7.7 (m, 30H, Ph_3NPPh_3), 3.93 (d, J_{H-P} = 1.8 Hz, 5H, C_5H_5), 1.45 (m, 6H, PCH_2CH_3), 1.0 (m, 9H, PCH_2CH_3). $^{31}P\{^1H\}$ NMR (THF-d_8): 89.5 (s, 1P, PEt_3), 21.8 (s, 1P, PPN). IR (Nujol): 1672, 1755 cm^{-1}.

$CpCr(CO)_2PEt_3$-Et_4N^+ (1e(Et_4N)). The synthesis followed the procedure used for the $P(OMe)_3$-substituted analogue and yielded orange-yellow prisms (78%). Anal. Calcd for $C_{21}H_{40}CrNO_2P$: C, 59.84; H, 9.56; N, 3.32. Found: C, 59.55; H, 9.44; N, 3.66. ^1H NMR (THF-d_8): 4.02 (d, J_{H-P} = 1.8 Hz, 5H, C_5H_5), 3.45 (m, 8H, CH_3CH_2N), 1.44 (m, 6H, PCH_2CH_3), 1.31 (t, J_{H-H} = 7 Hz, 12H, CH_3CH_2N), 1.0 (m, 9H, PCH_2CH_3). $^{31}P\{^1H\}$ NMR (THF-d_8): 88.8 (s). IR (Nujol): 1672, 1759 cm^{-1}.

Table I. Crystallographic Data

	$[NEt_4][CpCr(CO)_2PEt_3]$		
chem formula	$[C_{13}H_{20}CrO_2P][C_8H_{20}N]$	space group	$P2_1/n$
a, Å	12.430(1)	T, °C	−164
b, Å	14.917(2)	λ, Å	.71069
c, Å	13.218(2)	ρ_{calcd}, g cm^{-3}	1.218
β, deg	110.33(0)	μ(Mo K_α), cm^{-1}	5.67
V, Å^3	2298.40	R	.0326
Z	4	R_w	.0355
fw	421.52		
	$[Ph_3PNPPh_3][CpCr(CO)_2PEt_3]$		
chem formula	$[C_{13}H_{20}CrO_2P][C_{36}H_{30}NP_2]$	space group	$P2_1/c$
a, Å	16.618(2)	T, °C	−167
b, Å	14.665(2)	λ, Å	.71069
c, Å	17.993(3)	ρ_{calcd}, g cm^{-3}	1.264
β, deg	95.88(1)	μ(Mo K_α), cm^{-1}	4.01
V, Å^3	4361.78	R	.0391
Z	4	R_w	.0420
fw	829.86		

Structure Determinations.[16] (Data for the NEt_4 compound are given, followed by those for the PPN compound in parenthesis.) The crystal was affixed to a glass fiber using silicone grease and was then transferred to the goniostat where it was cooled to −164 °C (−167 °C) for characterization (Table I) and data collection ($6° < 2\theta < 45°$). A systematic search of a limited hemisphere of reciprocal space yielded a set of reflections which exhibited monoclinic ($2/m$) symmetry. The systematic extinction of $0k0$ for $k \approx 2n + 1$ and of $h0l$ for $h + l = 2n + 1$ uniquely identified the space group as $P2_1/n$ (No. 14). Data collection was undertaken as detailed in Table I. The structure was solved by the usual combination of direct methods and Fourier techniques. The Cr and P atoms were located in the initial E-map (MULTAN-78). The remaining non-hydrogen atoms were located in successive difference maps. Following the initial refinement, all of the hydrogen atoms were located in a difference map. The full-matrix least-squares refinement was completed using anisotropic thermal parameters on all non-hydrogen atoms and isotropic thermal parameters on the hydrogen atoms. The total number of variables was 396 (706), including the scale factor and an overall isotropic extinction parameter. The final difference map was essentially featureless; the largest peak was 0.30 (0.33) e/Å^3. The results

(15) Parker, V. D.; Handoo, K. L.; Roness, F.; Tilset, M. *J. Am. Chem. Soc.* **1991**, *113*, 7493.

(16) For general crystallographic details, see: Huffman, J. C.; Lewis, L. N.; Caulton, K. G. *Inorg. Chem.* **1980**, *19*, 1840.

Table II. Selected Bond Distances (Å) and Angles (deg) for $[NEt_4][CpCr(CO)_2PEt_3]$

Cr(1)–P(2)	2.2472(9)	Cr(1)–C(9)	2.222(3)
Cr(1)–C(3)	1.797(3)	Cr(1)–C(10)	2.195(3)
Cr(1)–C(5)	1.787(3)	Cr(1)–C(11)	2.194(3)
Cr(1)–C(7)	2.227(3)	O(4)–C(3)	1.196(4)
Cr(1)–C(8)	2.232(3)	O(6)–C(5)	1.202(4)
P(2)–Cr(1)–C(3)	90.29(9)	Cr(1)–C(5)–O(6)	178.16(26)
P(2)–Cr(1)–C(5)	90.04(10)	CTR[a]–Cr(1)–P(2)	123.00
C(3)–Cr(1)–C(5)	90.00(13)	CTR[a]–Cr(1)–C(3)	125.76
Cr(1)–C(3)–O(4)	178.63(25)	CTR[a]–Cr(1)–C(5)	126.76

[a] CTR indicates C_5 ring center of gravity.

Table III. Selected Bond Distances (Å) and Angles (deg) for $[PPN][CpCr(CO)_2PEt_3]$

Cr(1)–P(2)	2.2531(10)	Cr(1)–C(10)	2.221(3)
Cr(1)–C(3)	1.788(3)	Cr(1)–C(11)	2.201(3)
Cr(1)–C(5)	1.787(3)	P(18)–N(19)	1.5828(26)
Cr(1)–C(7)	2.214(3)	P(20)–N(19)	1.5837(26)
Cr(1)–C(8)	2.216(3)	O(4)–C(3)	1.201(4)
Cr(1)–C(9)	2.228(3)	O(6)–C(5)	1.199(4)
P(2)–Cr(1)–C(3)	90.92(10)	Cr(1)–C(5)–O(6)	177.44(27)
P(2)–Cr(1)–C(5)	89.69(10)	CTR[a]–Cr(1)–P(2)	119.80
C(3)–Cr(1)–C(5)	86.23(14)	CTR[a]–Cr(1)–C(3)	128.96
P(18)–N(19)–P(2)	140.73(18)	CTR[a]–Cr(1)–C(5)	129.25
Cr(1)–C(3)–O(4)	177.58(27)		

[a] CTR indicates C_5 ring center of gravity.

of the structure determination are shown in Tables II and III and Figures 1 and 2. Additional information is available as supplementary material.

Results

Solid-State Structural Studies. The X-ray diffraction studies reveal normal geometries for the Et_4N^+ (Figures 1 and 2) and PPN^+ (Figure 3) ions, together with anions of very similar structure. All bond lengths within the anions are identical to within 0.01 Å. Compared to $CpCr(CO)_3^-$,[17,18] the Cr/C distances are marginally shorter and the C/O distances are longer, consistent with considerable back-donation. The Cp ring rotational conformation is very similar in the two anions, and even the conformations of the PEt_3 groups are identical. This latter point suggests that the conformation is dictated by forces *within* the anion rather than by interionic steric factors (which will be different in salts with different cations). Angular parameters differ more than do the bond lengths between the two anions. Angles from the Cp ring center of gravity to P and to carbonyl carbons differ by less than 3.2°. The largest single difference between the two anions lie in the angle OC–Cr–CO, which is 90.00(13)° in the Et_4N^+ salt and 86.23(14)° in the PPN^+ salt.

Examination of unit cell drawings reveals no evidence for graphitic stacking of phenyl against Cp rings; were these present, they could be a mechanism for charge transfer.

The relative placement of anions and cations may be of relevance in understanding charge-transfer interactions. One measure of this is the list of distances between charge centers in these two salts (Table IV). This shows that the Cr/N distances are considerably shorter in the (noninteracting) Et_4N^+ salt than in the PPN^+ salt. This contrasts with the slightly higher density of the PPN^+ salt (1.264 vs 1.218 g/cm^{-3}) and is further evidence that there are no unusual cation/anion contacts in the PPN^+ salt. Finally, it is noteworthy that the N/Cr distances in $[PPN][CpCr(CO)_2PEt_3]$ are >1 Å longer than the shortest corresponding distances in salts shown by electrical conductivity measurements[5,6] to exhibit ion pairing in THF. In searching for the origin of the color of $[PPN][CpCr(CO)_2PEt_3]$, we have employed a variety of the other spectral techniques.

Infrared Spectral Analysis. Shown in Table V are the observed ν(CO) values for salts with two different cations in solvents of high (MeCN) and low (THF) dielectric constant. To evaluate the effect of anion electron density of these phenomena, we tabulate values for $CpCr(CO)_2L^-$ where L = CO, $P(OMe)_3$, PPh_3, and PEt_3. The data for $Cp^*Cr(CO)_3^-$ represents a case slightly more electron-rich than $CpCr(CO)_3^-$. As one proceeds down a column in this table, the anions become more electron-rich (i.e., more reducing). The following observations and conclusions may be made:

(1) All frequencies are independent of cation in MeCN. This suggests that separated ions are produced in every case in MeCN.

(2) No bands[19-21] for the neutral radical $CpCr(CO)_2L$ are seen. Such species are absent in these solutions (or are below a detection level of 1%).

(3) The observation of three bands for $Et_4NCpCr(CO)_3$ (and the Cp* analog) in THF demonstrates ion pairing with distortion from local C_{3v} symmetry. However, the higher frequency is essentially identical in THF and in MeCN. Likewise, the average of the two lower frequencies in THF is essentially identical to the frequency of the *E* vibration in MeCN. Taken together, this indicates that ion pairing in this compound degrades symmetry without altering C/O force constants and bond strengths. Thus, no charge transfer is implied in the $NEt_4(Ring)Cr(CO)_3$ (Ring = Cp and Cp*) ion pairs. Ion pairing here is essentially electrostatic in nature.

(4) More generally, the vibrational frequencies of the Et_4N^+ compounds are identical in THF and MeCN for all L except PEt_3, where the values in THF are slightly higher. Except for L = PEt_3, charge transfer to Et_4N^+ is essentially absent.

(5) In contrast to item 4 above, ν(CO) values of the PPN^+ salts are significantly higher in THF than in MeCN, and the disparity (for given L) increases as the anion is more electron-rich. This is consistent with the ion-pairing phenomenon in THF involving significant charge transfer from the anion to the PPN^+ cation. Such charge transfer essentially vanishes in the least reducing anion, $CpCr(CO)_3^-$.

(6) Comparison of the values for the two $CpCr(CO)_2PEt_3^-$ compounds in THF shows significantly more charge transfer to PPN^+ than to Et_4N^+.

The study of ion pairing involving $CpCr(CO)_2L^-$ species is further clarified because the neutral species $CpCr(CO)_2PPh_3$ is a persistent radical, and thus both its CO stretching frequencies and its X-ray diffraction structure are established. The only unusual structural feature of $CpCr(CO)_2(PPh_3)^q$ for $q = 0$ is that the angle OC–Cr–CO is 80.9(1), which is 9.1° smaller[19,22] than when $q = -1$. Our observation that ∠OC–Cr–CO is 86.23(14)° in $[PPN][CpCr(CO)_2PEt_3]$ thus takes on added significance in indicating some fractional degree of charge transfer. The average ν(CO) value for $CpCr(CO)_2(PPh_3)^q$ is 139 cm^{-1} higher for q = 0 than for $q = -1$. The rise in the average ν(CO) for $[PPN][CpCr(CO)_2PEt_3]$ in THF relative to the value in MeCN (15 cm^{-1}) permits (by linear interpolation) an approximation of 15/139 × 100 or 11% charge transfer from $CpCr(CO)_2PEt_3^-$ to PPN^+. This conclusion is in satisfactory agreement with the observed reduction in the angle OC–Cr–CO in the PPN compound.

NMR Studies. Since the above spectral probes revealed the occurrence of charge transfer, we also investigated the NMR spectroscopy of both PEt_3 derivatives in THF-d_8. Both salts show a single $^{31}P\{^1H\}$ NMR signal for the $CpCr(CO)_2PEt_3^-$ ion, with the chemical shift of the PPN^+ compound being 0.70 ppm to low-field of that of the Et_4N^+ salt. The PPN^+ salt also shows

(17) Rohrmann, J.; Herrmann, W. A.; Herdtweck, E.; Riede, J.; Sergeson, G. *Chem. Ber.* **1986**, *119*, 3544.

(18) Feld, R.; Hellner, E.; Klopsch, A.; Dehnicke, K. *Z. Anorg. Allg. Chem.* **1978**, *442*, 173.

(19) Cooley, N. A.; Watson, K. A.; Fortier, S.; Baird, M. C. *Organometallics* **1986**, *5*, 2563.

(20) Cooley, N. A.; MacConnachie, P. T. F.; Baird, M. C. *Polyhedron* **1988**, *7*, 1965.

(21) Baird, M. C. *Chem. Rev.* **1988**, *88*, 1217.

(22) The invariance of the CO intensities along the series L = PPh_3 or PEt_3 when $q = 0$ suggests no major changes occur in ∠OC–Cr–CO as L is varied.

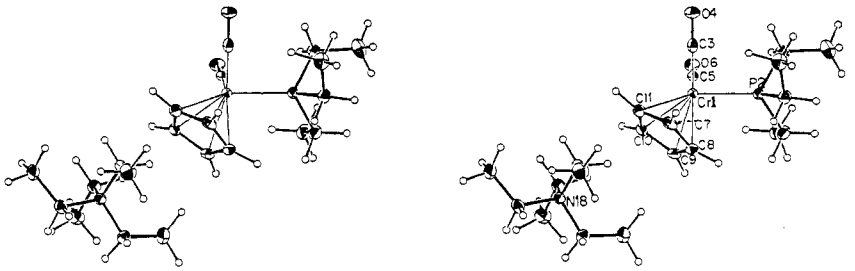

Figure 1. Stereo ORTEP drawing of the crystallographically-unique portion of $[NEt_4][CpCr(CO)_2PEt_3]$, showing selected atom labeling.

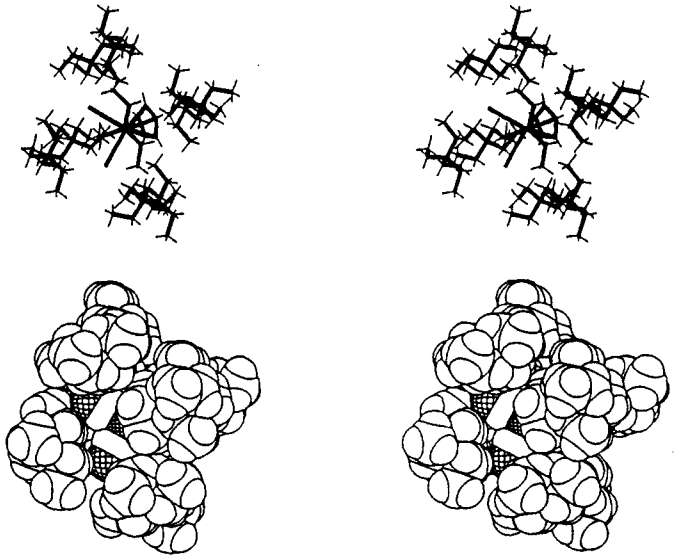

Figure 2. Stereo stick figure and space-filling drawing of one $CpCr(CO)_2PEt_3^-$ unit and eight adjacent symmetry-related Et_4N^+ ions.

a sharp signal due to the cation at 21.8 ppm, which is 0.1 ppm to high-field of that of (PPN)Cl in THF. There is thus clear but modest (<1 ppm) ^{31}P NMR evidence for ion pairing (chemical shift dependence on counterion) but no evidence for net paramagnetism (from charge transfer) in the ion pair in these solutions.

Electronic Spectra of Charge-Transfer Complexes. (a) Solvatochromism. With the exception of **1d**(Et_4N) which was red-brown, all salts of the tetraethylammonium cation were yellow, crystalline materials. On the other hand, all PPN salts except **1a**(PPN) formed deeply colored crystals; the colors ranged from orange-red for **1b** to almost black for **1e**. The colors persisted in THF solutions. The electronic spectra of all complexes were recorded in THF and are listed in Table VI. In all cases, no well-defined maxima were observed in the visible region, and therefore λ_{200} values, defined as the wavelengths for which the molar extinction coefficients ϵ were equal to 200, were measured. The absorption bands showed tailing well beyond these values; for 1 mM **1e**(PPN) in THF, the value for ϵ was ca. 17 at λ = 800 nm. The data in the table show that there is a semiquantitative correlation between the red shift observed in λ_{200} when the Et_4N^+ counterion is replaced by PPN^+ and the reduction power of the metal anion. This is in agreement with Mulliken's original formulation of electron donor–acceptor interactions.[23]

When the THF solvent is replaced with acetonitrile, the intense colors of the PPN^+ salts are extinguished (the color of **1d**(PPN) remains but λ_{200} is blue-shifted), leaving them identical to those of acetonitrile solutions of the Et_4N^+ salts. This solvatochromic behavior is in accord with reports by Kochi[2] and others[24] and indicates the breaking up of the contact ion pairs that exist in THF and that allow for the charge-transfer interaction for the proper donor–acceptor combinations.

(23) (a) Mulliken, R. S. *J. Am. Chem. Soc.* **1952**, *74*, 811. (b) Mulliken, R. S.; Person, W. B. *Molecular Complexes*; Wiley: New York, 1969.
(24) Schramm, C.; Zink, J. J. *J. Am. Chem. Soc.* **1979**, *101*, 4554.

(b) Salt Effect of Added $Bu_4N^+PF_6^-$. A similar effect was noted when moderate amounts of $Bu_4N^+PF_6^-$ were added to solutions of **1e**(PPN) in THF. The addition of 1 equiv of $Bu_4N^+PF_6^-$ led to a ca. 50% reduction of the absorptivity at λ_{200} (at which **1e**(Et_4N) did not absorb), and a bleaching of the color was visually discernible. Increasing amounts of $Bu_4N^+PF_6^-$ led to a further, roughly linear reduction in the intensity of the color. No such effect was observed when $PPN^+PF_6^-$ was added to the solution instead of $Bu_4N^+PF_6^-$. The effect is in agreement with the establishing of the following ion-exchange equilibrium (eq 1), the value of K_{eq} being essentially equal to unity.

$$PPN^+CpCr(CO)_2PEt_3^- + Bu_4N^+PF_6^- \overset{K_{eq}}{\rightleftharpoons} Bu_4N^+CpCr(CO)_2PEt_3^- + PPN^+PF_6^- \quad (1)$$

The salt effect was also observable by IR spectroscopy. Thus, a THF solution of **1e**(PPN) displayed ν(CO) bands at 1699 and 1774 cm^{-1}. The addition of 1 equiv of $Bu_4N^+PF_6^-$ caused a shift to 1693 and 1770 cm^{-1}. A significant broadening of both bands was observed, but separate peaks due to charge-transfer and non-charge-transfer species could not be resolved. With 10 equiv of $Bu_4N^+PF_6^-$ added, the IR spectrum was indistinguishable from that of **1e**(Et_4N) at 1686 and 1766 cm^{-1}, and both bands had sharpened again.

Electrochemical Behavior of 1a–e(Et_4N), 1a–e(PPN), and (PPN)PF_6. The electrochemical behavior of the anions **1a–e** and closely related analogues has been recently described by us and others.[25] In acetonitrile/0.1 M $Bu_4N^+PF_6^-$, chemically-reversible one-electron oxidation processes take place to give the persistent chromium-centered radicals. The weakness[26] of the chromium–chromium bonds that *would* result from radical dimerizations ensures that monomeric radicals are the predominant species in solution, allowing for the unusual observation of *reversible* oxidations of the anions. The reversible oxidation potentials for these processes, taken as the midpoints between the anodic and cathodic peak potentials, are listed in Table VI. The electron-donating capability of Cp* compared with Cp is quite evident, as is the increasing electron-donating power of the PR_3 ligands in the order $CO < P(OMe)_3 < PPh_3 < PEt_3$. This ranking is qualitatively in agreement with the trends observed in the positions of the infrared ν(CO) absorption bands and in the magnitude of the charge-transfer red shifts of the PPN salts of the anions.

The electrochemical behavior of **1e**(Et_4N) and **1e**(PPN) was briefly investigated in THF/0.1 M $Bu_4N^+PF_6^-$. Reversible waves were observed in this solvent, too. However, no difference was found in the oxidation potentials for the two. This was anticipated, considering the observed effect (eq 1) of added excess $Bu_4N^+PF_6^-$ to THF solutions of **1e**(PPN). The supporting electrolyte effectively breaks up the charge-transfer ion pair and precludes the observation of any effect of the charge-transfer interaction.

(25) (a) O'Callaghan, K. A. E.; Brown, S. J.; Page, J. A.; Baird, M. C.; Richards, T. C.; Geiger, W. E. *Organometallics* **1991**, *10*, 3119. (b) Madach, T.; Vahrenkamp, H. *Z. Naturforsch.* **1978**, *33B*, 1301.
(26) Watkins, W. C.; Jaeger, T.; Kidd, C. E.; Fortier, S.; Baird, M. C.; Kiss, G.; Roper, G. C.; Hoff, C. D. *J. Am. Chem. Soc.* **1992**, *114*, 907.

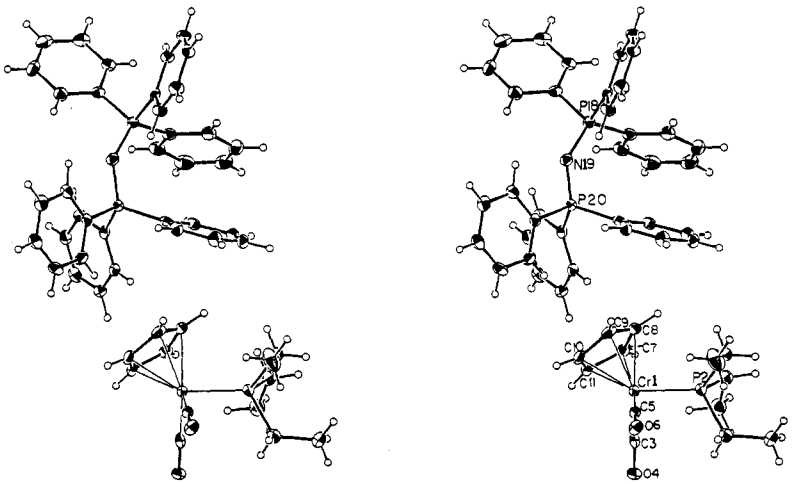

Figure 3. Stereo ORTEP drawing of the crystallographically-unique portion of the structure of $[Ph_3PNPPh_3][CpCr(CO)_2PEt_3]$, showing selected atom labeling.

Table IV. Cr···N Distances Less Than 10 Å in $[Cat][CpCr(CO)_2PEt_3]$

$Cat^+ = Et_4N^+$	$Cat^+ = Ph_3PNPPh_3^+$	$Cat^+ = Et_4N^+$	$Cat^+ = Ph_3PNPPh_3^+$
5.61	8.41	8.21	9.66
5.85	9.37	9.22	9.79
6.12	9.46	6.30	9.53
9.98	9.89		

Table V. C/O Infrared Stretching Frequencies (cm^{-1})[a]

	Et_4N^+		PPN^+	
	THF	MeCN	THF	MeCN
$CpCr(CO)_3^-$ (**1a**)	1888[b]	1890	1890	1890
	1772[b]	1772	1776	1773
	1761[b]			
$Cp^*Cr(CO)_3^-$ (**1b**)	1871	1870	1872	1870
	1759	1754	1760	1754
	1748			
$CpCr(CO)_2P(OMe)_3^-$ (**1c**)	1800	1800	1807	1801
	1720	1720	1731	1721
$CpCr(CO)_2PPh_3^-$ (**1d**)	1780	1780	1790	1780
	1704	1704	1718	1705
$CpCr(CO)_2PEt_3^-$ (**1e**)	1766	1763	1774	1762
	1686	1682	1699	1682

[a] 20 mM solutions unless otherwise noted. [b] Saturated solution.

Table VI. Electronic Spectroscopic and Redox Data for Cyclopentadienylchromium Anions **1a–e** in THF[a]

chromium anion	λ_{200}[a] for counterion = Et_4N^+	λ_{200}[a] for counterion = PPN^+	$E_{ox}(M^-)$, V vs Fc[b]
$CpCr(CO)_3^-$ (**1a**)			−0.69[c]
$Cp^*Cr(CO)_3^-$ (**1b**)	425	454	−0.83[c]
$CpCr(CO)_2P(OMe)_3^-$ (**1c**)	420	441	−1.11[c]
$CpCr(CO)_2PPh_3^-$ (**1d**)	575	632	−1.29[c]
$CpCr(CO)_2PEt_3^-$ (**1e**)	456	597	−1.51[c]

[a] Wavelengths (nm) at which 1.0 mM solutions give molar extinction coefficients equal to 200 (see text for explanation). [b] Reversible oxidation potential for the anion in acetonitrile/0.1 M $(Bu_4N)PF_6$, 25 °C. [c] From ref 7.

The electrochemical behavior of $PPN^+PF_6^-$ in THF/0.1 M $Bu_4N^+PF_6^-$ was investigated by derivative cyclic voltammetry[27] in order to quantify the acceptor properties of the cation. At ambient temperature, the reduction of PPN^+ appeared as an irreversible wave. However, cooling the system to 0 °C caused the reduction to exhibit significant chemical reversibility. At a voltage sweep rate v = 1.0 V/s, the reversible potential for the $PPN^+/PPN^\cdot$ couple, taken as the midpoint between the cathodic and anodic peak potentials, was measured as −2.64 V vs the ferrocene/ferrocenium (Fc) couple. Under these conditions, the cathodic to anodic derivative peak current intensity was ca. 0.75 when the voltage scan was reversed at a potential 190-mV cathodic of the reduction peak potential. The fate of the $PPN^\cdot$ radical following its moderately slow (on the CV time scale) subsequent chemical reaction was not investigated.

Effect of Supporting Electrolyte Cation: Electrochemistry of 1a(PPN) and 1e(PPN) in THF/(PPN)PF_6. It was reasoned that if the charge-transfer interaction in **1e**(PPN) significantly led to a reduction in the electron density at the metal center, then the oxidation potential of **1e**(PPN) might be significantly higher in a medium that preserved the charge-transfer interaction than in one in which it was disrupted. In the case that extensive and/or rapid contact ion pair dissociation takes place, oxidation of the solvent-separated anion could, however, occur in both media. For reasons already addressed, acetonitrile or THF/$Bu_4N^+PF_6^-$ were not viable choices for investigating this phenomenon, but the obvious choice for the medium would be THF/$PPN^+PF_6^-$. The solubility of $PPN^+PF_6^-$ in THF was lower than desirable for a good electrolyte, amounting to ca. 0.018 M at 30 °C. This led to a rather resistive medium. In spite of this, by applying a suitably high iR compensation with the positive-feedback circuitry of the potentiostat, acceptable voltammograms were obtained. Following the recommendations of others,[28] an iR compensation amounting to ca. 85% of the compensation that caused the circuitry to oscillate was chosen. Thus, the anodic to cathodic peak separation for the ferrocene/ferrocenium couple was measured to 81 ± 4 mV at a sweep rate v = 1.0 V/s at a 0.4 mm diameter Pt disk electrode at 30 °C. In order to make meaningful comparisons of the charge-transfer interaction, **1a** (with essentially no interaction) and **1e** (with the maximum interaction) were chosen for making comparisons. Oxidation potentials were measured by using derivative cyclic voltammetry (DCV) since it is well documented that the accuracy with which CV peak potentials can be measured by DCV is far superior to that offered by ordinary CV.[29]

First, the oxidation potential of **1a**(PPN) was measured vs Fc (added as internal standard) in THF/saturated $PPN^+PF_6^-$ (assumed to be 0.018 M) and in THF/0.018 M $Bu_4N^+PF_6^-$. It was noted that a greater iR compensation was needed for the latter medium, indicating that the degree of dissociation of the

(27) (a) Ahlberg, E.; Parker, V. D. *J. Electroanal. Chem. Interfacial Electrochem.* **1981**, *121*, 73. (b) Parker, V. E. *Electroanal. Chem.* **1986**, *14*, 1.

(28) (a) Eliason, R.; Parker, V. D. *J. Electroanal. Chem. Interfacial Electrochem.* **1984**, *165*, 21. (b) *User's Guide* for EG&G-PAR Model 270 Electrochemical Analysis System, 1989.

(29) Ahlberg, E.; Parker, V. D. *Acta Chem. Scand., Ser. B* **1980**, *B34*, 53.

supporting electrolyte into conducting "free" ions is greater for $PPN^+PF_6^-$ than for $Bu_4N^+PF_6^-$. The poor conductivity in this latter medium led to a peak separation as high as 163 ± 3 mV for Fc. The oxidation potential for **1a**(PPN) in THF/saturated $PPN^+PF_6^-$ was −888 ± 1 mV vs Fc. These and following values represent the means with one standard deviation of measurements performed five times on freshly prepared solutions of the species involved. Similarly, in THF/0.018 M $Bu_4N^+PF_6^-$, **1a**(PPN) underwent oxidation at −920 ± 2 mV vs Fc. It is noteworthy that these data are very different from the potentials observed in acetonitrile/0.1 M $Bu_4N^+PF_6^-$, 0.69 V vs Fc. The difference may be attributed to the different charges present in the couples being compared. It is to be expected that the polarity increase (acetonitrile instead of THF) will tend to stabilize the high oxidation state for the Fc couple as compared with the low oxidation state for the $Cr^-/Cr^\bullet$ couple and both effects tend to narrow the potential difference between the two in a more polar medium. When the $Bu_4N^+PF_6^-$ concentration was increased to 0.1 M in THF (accompanied by proper adjustment of the *iR* compensation), **1a**(PPN) underwent oxidation at −836 ± 2 mV vs Fc. It was noted here that, relative to the experimentally used Ag/Ag^+ reference, the oxidation potential of **1a** was unchanged by the increase in $Bu_4N^+PF_6^-$ concentration, and so it was the Fc potential that gave rise to the difference in E_{ox}(**1a**) vs Fc.

We now attempted to accurately determine the difference in reversible oxidation potentials of **1e**(PPN) vs **1a**(PPN) in THF. Solutions were prepared that contained roughly equimolar amounts of the two. The color of the solution in THF/0.018 M $PPN^+PF_6^-$ clearly indicated that the charge-transfer interaction was intact. In contrast, the solution obtained in THF/0.018 M $Bu_4N^+PF_6^-$ was pale yellow. The peak potentials for the oxidation of **1a**,**e** and for the reductions of their radicals were accurately measured by DCV. Because **1a**,**e** represent species of like charges, solvation effects of the anion and neutral states should cancel and direct comparisons of the oxidation potential differences of the two in the chosen THF media should be meaningful. The chemically reversible wave due to **1e**(PPN) displayed a peak-to-peak separation of 140–175 mV in THF/0.018 M $PPN^+PF_6^-$ and THF/0.018 M $Bu_4N^+PF_6^-$. The value depended on the electrode history, such as number of scans performed before actual measurement after polishing the electrode. The reversible potentials (midpoint between anodic and cathodic peaks) were however highly reproducible and also were dependent on the identity of the electrolyte. It was found that E_{ox}(**1e**(PPN)) − E_{ox}(**1a**(PPN)) was −837 ± 3 mV in THF/0.018 M $PPN^+PF_6^-$, −807 ± 2 mV in THF/0.018 M $Bu_4N^+PF_6^-$, and −799 ± 1 mV in THF/0.1 M $Bu_4N^+PF_6^-$. The data indicate that the oxidation of **1e**(PPN) is *harder* in THF/$Bu_4N^+PF_6^-$ (negligible charge transfer) than in THF/$PPN^+PF_6^-$ (charge transfer extant), contrary to our expectations.

Discussion

Kochi emphasized[1] the close relationship between reductant and nucleophile. In the limiting case of an electrophile which shows extreme resistance to being reduced (e.g., the alkali metal cations), it is best to think of the cation/anion ("ion-pair") interactions as lying somewhat on a continuum between Coulomb attraction among unit point charges and Lewis acid/base interaction between alkali metal valence orbitals and anion lone pairs on the ligand. Metal–metal dative interaction involving alkali metal/transition metal carbonyl compounds has not been observed. Either of these involves symmetry reduction of the anion, perhaps accompanied by change in the vibrational force constants (bond strengths) in the anion.

As the cation becomes more easily reducible (e.g., Tl^+, Cu^+, or Ag^+), electron transfer becomes a new element of the ion-pairing phenomenon, and thus a charge transfer between ions becomes a special case of ion pairing.[24,30,31] The limiting case occurs when charge transfer occurs to the extent that the original cation and anion form direct metal/metal bonds.[30,32]

When the cation lacks low-lying empty orbitals (e.g., Cp_2Co^+) or lacks a metal (ER_4^+ with E = N, P, or As or $Ph_3PNPPh_3^+$), charge transfer is not anticipated on the basis of prior observations.[1-3,5,33-36] However, the very sensitive probes of visible/UV and infrared spectroscopy (primarily ν(CO)) reveal the occurrence of charge transfer involving highly reducing anionic transition-metal complexes, even when the free energy change for full electron transfer is highly unfavorable. This report is the first observation of a significant rise in ν(CO) as a result of charge transfer. In a similar manner, Kochi[4] has used the N/O stretching frequency to quantitate charge transfer in [NO^+; arene] charge-transfer complexes. Likewise, the C≡C stretching vibration in certain organic donor and acceptor molecules has been used to gauge the degree of charge transfer in their solid-state charge-transfer complexes.[37,38]

Although these spectroscopic probes support the occurrence of charge transfer in the solid state (as well as solution), the solid-state structure reveals no short *pairwise* cation/anion contacts or contacts which lead to angular distortions and serve to bring atoms of the PPN^+ cation in (weak) bonding distance to the metal of the anion. This is to be expected, since ion packing in the solid state is dictated by the demands of $\sim 10^{20}$ ions, which generally leads to placement of many counterions about each anion.[10] The solution geometry, involving as it does a single[5] cation/anion pair, could involve a more spatially-limited contact geometry. For example, the drawing presented[2] for $Cp_2Co^+I^-$ conveys the idea that a pairwise interaction exists in the solid state. In fact, there are four identical Co/I distances of 4.75 Å in the mirror plane containing cobalt and parallel to both Cp rings. In addition, there are two identical Co/I distances of 5.83 Å, where these iodides lie on the C_5 axis of the cation but on the side of the Cp opposite the cobalt. Finally, there are eight identical Co/I separations of 8.89 Å. In a similar manner, for $[Cp_2Co]$-$Co(CO)_4$ in the solid state, there are four pairs of Co(I)/Co(−I) distances ranging from 5.42 to 6.88 Å. Under these circumstances, then, it cannot generally be expected that (low dielectric) solution and solid-state ion pairs will show identical spectra.

This is the case with our data on $[Cat][CpCr(CO)_2PEt_3]$ in that the CO frequencies in Nujol drop to 1759 and 1672 cm^{-1} for the Et_4N^+ case and to 1755 and 1672 cm^{-1} for the PPN^+ case. Since ν(CO) values of even neutral, molecular transition-metal carbonyls are always observed to be lower in the solid state than solution, the observed reductions in ν(CO) cannot simply be interpreted in terms of greater charge transfer in the solid state than in THF. However, the proximity of the solid-state values in the Et_4N^+ and PPN^+ solids suggests charge transfer of these two salts may be more similar in the solid lattice than in THF solution.

To put the present work in a proper context, a few additional comparisons are useful. Non-Lewis acid cations have been reported to perturb ν(CO) in $Et_4NV(CO)_5PnBu_3$[34] and in

(30) Ernst, R. D.; Marks, T. J.; Ibers, J. A. *J. Am. Chem. Soc.* **1977**, *99*, 2090.
(31) Schussler, D. P.; Robinson, W. R.; Edgell, W. R. *Inorg. Chem.* **1974**, *13*, 153.
(32) Klüfers, P. *Angew. Chem., Int. Ed. Engl.* **1984**, *23*, 307 and references cited therein.
(33) Darensbourg, M. Y.; Borman, C. *Inorg. Chem.* **1976**, *15*, 3121.
(34) Darensbourg, M. Y.; Hanckel, J. M. *Organometallics* **1982**, *1*, 82.
(35) Darensbourg, M. Y.; Jimenez, P.; Sackett, J. R.; Hanckel, J. M.; Kump, R. L. *J. Am. Chem. Soc.* **1982**, *104*, 1521.
(36) As this work was being completed, it has been reported that even the less electron-rich anions $Co(CO)_4^-$, $Mn(CO)_5^-$, and $HFe(CO)_4^-$ show evidence of charge-transfer interactions with PPh_4^+, $PPh_3(CH_2Ph)^+$, and SPh_3^+ cations. Such pairs are, however, "unperturbed" by the IR criterion and also show only a broad tail in their visible spectrum. See: Wei, C. H.; Bockman, T. M.; Kochi, J. K. *J. Organomet. Chem.* **1992**, *428*, 85.
(37) Van Duyne, R. P.; Cape, T. W.; Suchanski, M. R.; Siedle, A. R. *J. Phys. Chem.* **1986**, *90*, 739.
(38) Tanaka, M.; Shimizu, M.; Saito, Y.; Tanaka, J. *Chem. Phys. Lett.* **1986**, *125*, 594.

$Me_4NCpMo(CO)_3$.[18] The solid-state structure of $Me_4NCpCr(CO)_3$ shows one Me_4N^+ hydrogen within van der Waals contact of an oxygen. Finally, the ion-pair dissociation constant of $CpMo(CO)_3^-$ is about the same[35] (10^{-6} M) for Me_4N^+, for PPN^+, and for Na^+; this would seem to suggest that the constant is dominated by charge and only slightly influenced by Lewis acidity.

It is now established that there are two structural forms for the PPN^+ cation: linear and bent (~140°) at nitrogen.[39,40] These correspond to two Lewis structures A and B. From the available

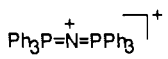

A

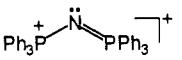

B

structures, there is no clear correlation between PPN^+ structure and properties of the counterion. Indeed, in a salt of an oxomolybdate cluster anion, *both* linear and bent forms are found in distinct sites in the unit cell.[39] Since the PPN^+ cation in the solid reported here has no unusual structural features compared to the many examples of form *B*, we are forced to conclude that any charge transfer in $[PPN][CpCr(CO)_2PEt_3]$ has no structural consequences for PPN^+ and that charge transfer is not a factor in determining the occurrence of form *A* vs *B*.

While the PPN^+ cation has been widely employed in metal carbonyl anion chemistry, its role was traditionally attributed to good size match[9,10] for crystal growth behavior and *lack* of the symmetry perturbing "interactions" found for alkali metal cations. M. Darensbourg has summarized[5,6] and expanded the evidence that the PPN^+ cation exerts a "protecting" influence on its counteranion: solid salts containing metal carbonyl anions exhibit a reduced sensitivity to decomposition/reaction from O_2 and perhaps even H_2O, in comparison to their alkali metal salts. Darensbourg pointed out that this effect persists in solution and measured ion-pairing association constants of nearly 10^4 in THF. This stabilizing effect was attributed[6] to "...a physical, covering type of protection towards its associated anion, even in solution." On the basis of the results we report here, we suggest that this protective effect is due in part to the charge redistribution implicit in the formation of a charge-transfer pair: the anion becomes less reducing in the charge-transfer pair, and thus is less sensitive to external oxidants and electrophiles. Distinct colors for PPN vs alkali metal salts have not been explicitly mentioned in the literature, but deserve scrutiny in the future. While the dramatic color differences reported here may arise because of the very electron-rich (i.e., reducing) character of $CpCr(CO)_2PR_3^-$ ions (which *include* R = Ph), we feel that the electron-acceptor character of $Ph_3PNPPh_3^+$ is now established and must be considered in future work, including photochemical reactivity studies of PPN^+ salts.[41,42]

Acknowledgment. This work was supported by the U.S. National Science Foundation, by Statoil under the VISTA program, and by NATO (Grant No. CRG 910473).

Supplementary Material Available: Listings of full crystallographic details, fractional coordinates, and anisotropic thermal parameters (10 pages); listings of observed and calculated structure factors (23 pages) for $[Cat][CpCr(CO)_2PEt_3]$ (Cat = Et_4N^+ and $Ph_3PNPPh_3^+$). Ordering information is given on any current masthead page.

(39) Kirtley, S. W.; Chanton, J. P.; Love, R. A.; Tipton, D. L.; Sorrell, T. N.; Bau, R. *J. Am. Chem. Soc.* **1980**, *102*, 3451.

(40) Wilson, R. D.; Bau, R. *J. Am. Chem. Soc.* **1974**, *96*, 7601.

(41) See, for example: Faltynek, R. A.; Wrighton, M. S. *J. Am. Chem. Soc.* **1978**, *100*, 2701.

(42) **Note added in proof**: It appears that the orange PPN^+ salt of $(C_5Ph_5)Cr(CO)_3^-$ (cf. the yellow sodium salt) may also display charge transfer. Hoobler, R. J.; Hutton, M. A.; Dillard, M. M.; Castellani, M. P.; Rheingold, A. L.; Rieger, A. L.; Rieger, P. H.; Richards, T. C.; Geiger, W. E. *Organometallics* **1993**, *12*, 116.